Precipitation Flux Climatology of the Free Atmosphere[1]

MICHAEL HANTEL

Meteorologisches Institut der Universität Bonn, Federal Republic of Germany

HERBERT LANGHOLZ

Deutscher Wetterdienst, Offenbach, Federal Republic of Germany

(Manuscript received 2 November 1976, in revised form 2 February 1977)

ABSTRACT

The diabatic heating of the atmosphere can be very closely represented by the convergence of a vertical energy flux. It consists of two components: the flux of net radiation and the flux of precipitation. The latter comprises the vertical flux of water in condensed form (rain, snow, ice). The concept of precipitation flux is investigated employing the zonal mean equation of potential heat. Input data are radiation flux from a model, adjusted at the top and bottom of the atmosphere with observed data; horizontal advective heat flux convergence and heat storage with the data of the MIT Library; and vertical subsynoptic eddy flux of sensible heat (a small quantity) from a parameterization. Output is the precipitation flux in the free atmosphere. Time scale is 1 month, space domain is the zonal mean Northern Hemisphere.

The precipitation flux is downward everywhere. It is maximum in the tropics. Comparison of the flux across the 1000 mb level with the observed surface precipitation shows satisfactory agreement. The balance in the potential heat equation is largely between radiation and precipitation; thus the atmosphere can be characterized by an approximate radiative-precipitative equilibrium. The accuracy of the method (± 10 W m^{-2}) depends critically on the validity of the radiation data.

1. Introduction

This study is a contribution to the quantitative climatology of the free atmosphere. We want to investigate the condensational heating, which cannot be measured directly, as close to observations as possible. This quantity is an important climate factor and thus deserves particular attention. We shall treat condensation as a vertical flux divergence and shall study the zonal mean patterns of the precipitation flux.

The condensational heating of the zonal mean atmosphere has been studied quantitatively by Newell *et al.* (1974). These authors used surface precipitation data along with cloud statistics at extratropical latitudes and model vertical wind profiles at the equator to obtain vertical distributions of latent heat release (their Fig. 7.16); this approach does not need radiation information. On the other hand, Thommes (1974) entered the first law of thermodynamics with observed horizontal fluxes of sensible heat and with model radiational heating and came up with an annual map of the condensation rate throughout the northern atmosphere; this approach does not need precipitation information.

In the present study we consider the condensation term, in analogy to the radiational heating, as divergence of the vertical precipitation flux. The precipitation flux concept has been introduced recently (Hantel, 1974) and was further discussed from the energy budget and streamfunction viewpoints (Hantel and Peyinghaus, 1976; Hantel *et al.*, 1976). We determine the precipitation flux from the conservation equation for potential heat (equivalent to dry static energy) which is similar to the method of Thommes; in particular, we shall specify radiation but do not require input precipitation. Domain is the northern atmosphere in a vertical-meridional section (0–1000 mb, 10°S–90°N; time-scale, 1 month).

In the following we shall briefly recapitulate the basic equations (Section 2) and specified data (Section 3) and then present (Section 4) and discuss (Section 5) seasonal patterns of the precipitation flux.

2. The precipitation flux concept

The familiar equations for mechanical and thermal energy read

$$\rho \frac{d}{dt}(k+\Phi)+\nabla\cdot(p\mathbf{v})=p\nabla\cdot\mathbf{v}, \tag{2.1}$$

$$\rho \frac{d}{dt}(c_v T)-\rho Q=-p\nabla\cdot\mathbf{v}. \tag{2.2}$$

[1] Based on a paper by M. Hantel and H. Langholz entitled "Radiative-precipitative equilibrium of the northern atmosphere", presented at the International Conference on Cloud Physics, 26–30 July 1976, Boulder, Colo.; and on a paper by H. Langholz entitled "Zonal mean precipitation flux in the northern atmosphere", presented at the International Conference on Simulation of Large-Scale Atmospheric Processes, 30 August–4 September 1976, Hamburg, Germany.

The symbols ρ, t, k, Φ, p, $\mathbf{v}$, c_v, T, Q, ∇ denote, respectively, density, time, kinetic energy, geopotential, pressure, three-dimensional velocity vector, specific heat at constant volume, temperature, diabatic heating and the nabla operator. We interpret the dependent variables as averages over a sufficiently large scale, say, 0.1–1 km in space and 1–10 min in time. This is equivalent to saying that we have neglected viscosity and Reynolds stress terms in (2.1) and (2.2); however, this does not affect the points we want to make. For a more complete derivation see Hantel *et al.* (1976).

If condensation is absent the diabatic heating is caused by radiation and conduction. Van Mieghem (1973) has introduced the notion

$$-\rho Q \equiv \nabla \cdot \mathbf{w} \tag{2.3}$$

which treats the diabatic heating as the divergence of the radiative (plus conductive) energy flux vector $\mathbf{w}$. Thus the total energy equation reads

$$\rho \frac{d}{dt}(k+\Phi+c_v T)+\nabla\cdot(p\mathbf{v}+\mathbf{w})=0. \tag{2.4}$$

The parameterization (2.3) is exact in the *dry case* since the atmosphere does not store electromagnetic energy. In the *moist case*, Q also comprises condensation which can be expressed by the local time change of the amount of condensed water (raindrop storage) plus the flux divergence of condensed water (see Kessler, 1969). For the present medium- to large-scale conditions we consider condensation as stationary and the three-dimensional precipitation flux vector as practically vertical in direction, in analogy to radiation. Consequently, we adopt (2.3) for the general moist case and write the diabatic heating as the divergence of the generalized heat flux vector (Hantel, 1974) as

$$\mathbf{w} \equiv \{0,\ 0,\ gH_R - gLH_C\}: \quad \left.\begin{matrix} H_R\ (\mathrm{J\ m^{-2}\ s^{-1}}) \\ H_C\ (\mathrm{kg\ m^{-2}\ s^{-1}}) \end{matrix}\right\}. \tag{2.5}$$

Here H_R is the vertical radiation flux and H_C the vertical condensation or precipitation flux. Gravity g has been introduced for convenient dimensions of H_R and H_C; L is the latent heat of condensation. The conductive heat flux is not included in $\mathbf{w}$; it is presumably small and will be absorbed into the advective heat flux discussed below. The precipitation flux comprises only the flux of water in condensed form but no vapor contribution.[2] The signs of the flux components are such that H_R and H_C are positive downward. Eq. (2.5) reflects a peculiarity of the vertical heat flux: if H_C is downward (positive) it acts as an upward (negative) heat flux, and vice versa. Thus the downward radiation flux and the downward precipitation flux combine in the global mean to an almost zero net heat flux $\mathbf{w}$.

[2] Note, however, that evaporation is considered as negative precipitation flux divergence and thus is implicitly contained in H_C.

3. Compilation of the precipitation flux

The total heat equation (2.4) is quite general. We shall apply it to the zonally symmetric case. Let us denote the zonal and time mean plus deviation by the familiar symbols (e.g., Oort and Rasmusson, 1971)

$$\text{zonal: } [\ ]+^*; \quad \text{time: } \bar{}+'. \tag{3.1}$$

The averaged equation (2.4) along with the approximation (2.5) then reads in pressure coordinates with $\omega \equiv dp/dt$:

$$\frac{\partial}{\partial t}[\bar{\Phi}+c_v\bar{T}]+\frac{\partial[\overline{vs}]\cos\phi}{\partial\eta}+\frac{\partial[\overline{\omega s}+g\overline{H_R}-gL\overline{H_C}]}{\partial p}=0, \tag{3.2}$$

where we have introduced

$$\left.\begin{aligned} s &\equiv \Phi+c_p T\ [\text{potential heat}] \\ \eta &\equiv a\sin\phi\ [\text{meridional coordinate}] \end{aligned}\right\} \tag{3.3}$$

and have neglected the kinetic energy k since it is small compared to s. The quantity s is often referred to as dry static energy. We integrate (3.2) with respect to pressure and solve for the precipitation flux. With the self-explanatory abbreviations

$$\left.\begin{aligned} \frac{1}{g}\frac{\partial}{\partial t}\int_0^p [\bar{\Phi}+c_v\bar{T}]dp &\equiv \mathrm{STOR} \\ \frac{1}{g}\frac{\partial}{\partial\eta}\left\{\cos\phi\int_0^p [\overline{vs}]dp\right\}+\frac{1}{g}[\overline{\omega s}] &\equiv \mathrm{ADV} \\ [\overline{H_R}]-[\overline{H_R}]_{p=0} &\equiv \mathrm{RAD} \\ L[\overline{H_C}] &\equiv \mathrm{PREC} \end{aligned}\right\}, \tag{3.4}$$

we obtain the balance

$$\boxed{\mathrm{STOR}+\mathrm{ADV}+\mathrm{RAD}\approx\mathrm{PREC}} \tag{3.5}$$

We shall use this formula to determine the unobservable PREC from the sum of the three observable quantities on the left.

Before continuing we shall mention an equivalent but less feasible method of determining H_C. The first law (2.2) can be written in the form

$$\frac{dc_p T}{dt}-Q=\frac{R\omega T}{p}, \tag{3.6}$$

where R is the gas constant. This yields in zonal mean

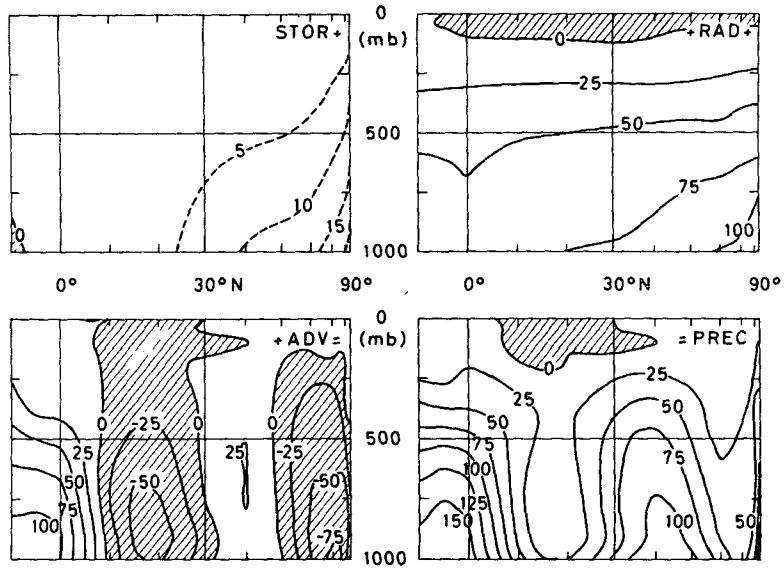

FIG. 1. Components of vertical heat flux (W m^{-2}) in the northern atmosphere, positive downward, valid for April. For definition of STOR, RAD, ADV, PREC, see Eqs. (3.4) and (3.5).

pressure coordinates

$$\frac{\partial}{\partial t}[c_p\bar{T}]+\frac{\partial[\overline{vc_pT}]\cos\phi}{\partial\eta}+\frac{\partial[\overline{\omega c_pT}+g\overline{H_R}-gL\overline{H_C}]}{\partial p}=\frac{R}{p}[\overline{\omega T}]. \quad (3.7)$$

This equation is equivalent to (3.2). The practical evaluation of (3.7), however, is hampered by the relatively large size of $(R/p)[\overline{\omega T}]$ which nevertheless is a poorly known quantity due to its significant subsynoptic eddy component. Test runs with (3.7) showed less satisfying results than with (3.2). Our calculations made with (3.2) proved to be almost independent of the eddy component of $[\overline{\omega s}]$.

For STOR and ADV in (3.5) we employ the zonal mean atmospheric circulation data of the MIT-Library, published by Oort and Rasmusson (1971). The data are monthly averages and are given on 11 pressure surfaces from 50 to 1000 mb with 5° latitude resolution. The horizontal flux of potential heat splits according to

$$[\overline{vs}]=[\bar{v}][\bar{s}]+[\bar{v}^*\bar{s}^*]+[\overline{v's'}] \quad (3.8)$$

(mean, standing eddy and transient eddy flux). Each of the three splits again into a geopotential and a sensible heat flux. The resulting six components of (3.8) are significant only on the synoptic scale. They are all listed separately in Oort and Rasmusson's tables. Thus the integrals in STOR and ADV could be simply compiled.

Concerning the vertical part ADV, it splits in a way similar to (3.8). The eddy terms (of which only the transient eddy is important) split again into a synoptic plus a boundary layer component. We have parameterized the synoptic component of $[\overline{\omega's'}]\approx c_p[\overline{\omega'T'}]$ according to Saltzman and Vernekar (1971) through the meridional transient eddy heat flux; the transient potential energy flux $[\overline{\omega'\Phi'}]$ has been neglected in analogy to the meridional fluxes for which $c_p[\overline{v'T'}]\gg[\overline{v'\Phi'}]$. Saltzman and Vernekar's formula is an overestimate in baroclinic zones and an underestimate in the tropics; however, $[\overline{\omega's'}]$ is relatively small so that the parameterization is not crucial. For a detailed discussion of $[\overline{\omega'T'}]$ see Hantel and Baader (1976).

The boundary layer flux component of $[\overline{\omega's'}]$ is of influence only in the lowest 100 mb. It was introduced by Newell *et al.* (1969) and was discussed by Thommes (1974). In the present study the boundary layer flux has been neglected except at the earth's surface where Budyko's (1963) sensible heat flux value (slightlys adjusted) were taken. For technical details of the compilation of STOR and ADV we refer to Langholz (1976).

Concerning RAD, we adopted the monthly radiation flux data from a recent modeling effort (Peyinghaus, 1974; Falconer and Peyinghaus, 1975). The fluxes from this model were compared with observations at the top and bottom of the atmosphere and showed satisfactory agreement (Hantel and Peyinghaus, 1976). However, there do not exist representative radiation flux measurements in any intermediate level. We consider this the one principal source of uncertainty in the present results.

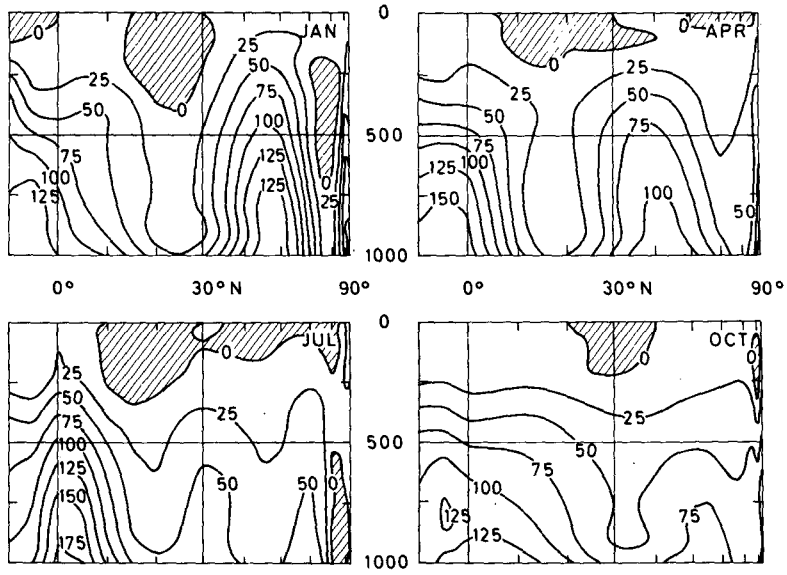

FIG. 2. Vertical precipitation flux (W m^{-2}) in the northern atmosphere for the central months of the seasons.

4. Results

The four terms of Eq. (3.5) are portrayed separately in Fig. 1 in vertical-meridional sections for April. The storage term is small over most of the Northern Hemisphere except in the highest latitudes. We note that STOR was inadvertently calculated with $\Phi+c_pT$ instead of $\Phi+c_vT$ which does not make much difference; in January and July, STOR is completely negligible. RAD represents a downward heat flux due to net radiation divergence, fairly uniformly distributed throughout the northern atmosphere. ADV represents a downward heat flux in the tropics and midlatitudes and an upward flux in the subtropics and polar latitudes.

Note that ADV does not simply show a uniform divergent area in the tropics and a uniform convergent area in the subtropics; this is only the case in October (not shown). In the other seasons the meridional potential heat flux, being positive throughout the Northern Hemisphere, has an intermediate maximum around 10°N and a minimum around 30°N which generates the secondary convergent area of ADV in the subtropics and the secondary divergent area of ADV in the extratropics up to 50°N (Fig. 1). This has already been indicated by Sellers (1965) and by Oort (1971; see curves labeled 4 in his Fig. 10). In other words, ADV exhibits a delicate balance between various energy transport mechanisms; this is an important factor for the meridional structure of the precipitation.

The resulting pattern of the precipitation flux shows positive values everywhere in the northern atmosphere, not only in April but throughout the year (Fig. 2). This is satisfying since only a net downward precipitation flux makes physical sense and indicates that the data from different sources entering the compilation of PREC fit reasonably together. The small negative patches in the upper atmosphere are presumably below the significance level. Very close to the earth's surface the patterns of Fig. 2 are uncertain due to the neglected boundary layer flux and further due to the non-identity of the earth's surface and the 1000 mb level.

Nevertheless, Fig. 2 reflects the climatological rainbelts in the deep tropics and in midlatitudes, and their seasonal fluctuation. The precipitation flux reaches high up into the upper troposphere with significant values of 25 units even across the 250 mb level, both in the tropics and midlatitudes. The winter midlatitude fluxes seem to be overestimated. This might be qualitatively explained by the following argument.

The meridional potential heat flux in subtropical latitudes is mainly accomplished by transient plus standing eddies; their contribution is about twice as large as the one by the mean meridional circulation (Oort, 1971; Figs. 4 and 5). The governing component of the eddy potential heat flux is the eddy flux of sensible heat. The latter is, to first order approximation, proportional to the scale of the horizontal wind. Now it is known that the radiosonde observing network tends to underestimate peak wind velocities. Consequently, correcting for such a systematic underestimate would increase the meridional potential heat flux in the subtropical jet latitudes. By raising $\partial[\overline{vs}]/\partial\eta$, this would act toward an increase of ADV in the subtropics south of the wind maximum, and toward a decrease in the extratropics north of the wind maximum, resulting in a more uniform pattern of PREC between 20°–50°N in winter. However, it is difficult to estimate this effect quantitatively.

5. Comparison with surface precipitation

The 1000 mb values of Fig. 2, reduced with the surface boundary layer flux, have been converted into rain flux dimensions and are presented in Fig. 3 along with independent estimates of surface precipitation from Möller (1951), the estimates of Rasmusson (see Newell *et al.*, 1972) which are based on synoptic-scale data of the water vapor transport and Budyko's (1963) evaporation estimates, and Jaeger's (1976) zonal averages from a comprehensive global budget of all available precipitation observations with 5° latitude and longitude resolution. In a recent study the overall error of contemporary hemispheric heat budget compilations was estimated to be of the order 10 W m^{-2} (Hantel, 1976) corresponding to about 1 g cm^{-2} $month^{-1}$; it has been entered in Fig. 3 as error limits of the dotted values.

In general, the coincidence in Fig. 3 is fair. The most intriguing discrepancies are visible in the winter midlatitudes where our estimates appear too high and in July in the subtropics where they appear too low. The July discrepancy is difficult to explain. Concerning January, we refer to the above remarks about the tendency of wind measurements to underestimate peak

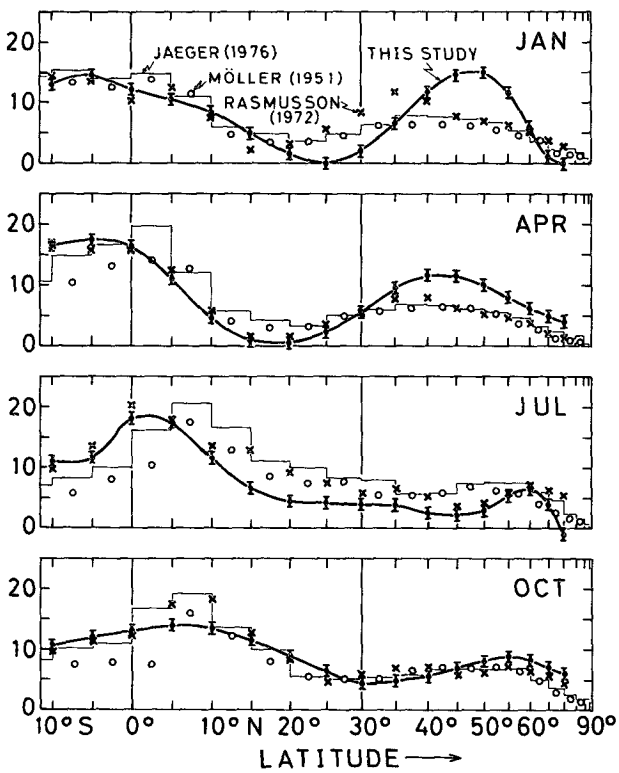

FIG. 3. Surface precipitation (g cm^{-2} $month^{-1}$): thick curve connecting solid dots with error limits (±1 g cm^{-2} $month^{-1}$) from present study, valid for 1000 mb; open circles from Möller (1951); crosses from Rasmusson (see Chap. 5 in Newell *et al.*, 1972); and thin histogram from Jaeger (1976). Data from Möller, Rasmusson and Jaeger are valid for the earth's surface.

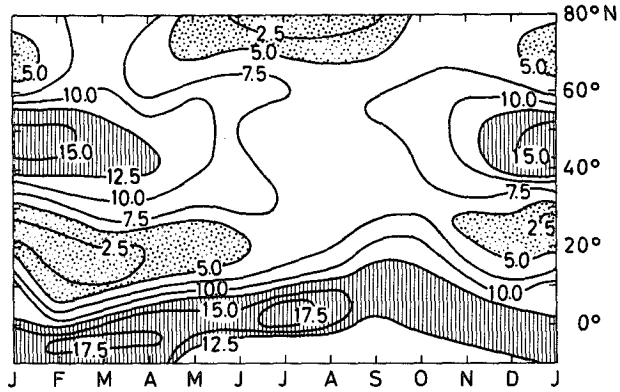

FIG. 4. Precipitation flux (g cm^{-2} $month^{-1}$) across 1000 mb in time-latitude section. Rain zones hatched, dry zones stippled.

velocities. Further, the "observed" extratropical precipitation in winter might be too low, due to strong wind influence on rain and snow gages; this effect can amount to more than 100% over Canada and Russia (see, for example, Hare and Hay, 1971).

An interesting analogy between our results and a recent statistical cloud model of Sasamori (1975) might be mentioned. Sasamori computed the surface precipitation for zonal mean global conditions, with the NCAR GCM data as input. His January curve seems also to overestimate in the 40°–50°N latitude belt the observed data of Schutz and Gates (1971) by some 100%. Since we consider our Fig. 3 largely as a consistency test for the precipitation flux concept, we are satisfied by the moderate fit of our results with independent estimates.

Another method which has been developed quite recently for the direct observation of surface rain flux might be worth mentioning. Rao *et al.* (1976) have published a satellite-derived rainfall atlas for 1973 and 1974 based on the Electrically Scanning Microwave Radiometer output, operating at 19.35 GHz, carried on board the Nimbus 5 satellite. The emerging brightness temperatures were calibrated, employing a Marshall-Palmer raindrop spectrum, into rainfall rates. This approach is limited to oceanic areas which must not be ice-covered. The resulting seasonal and zonal mean rainfall profiles up to about 60° latitude show general coincidence with our Fig. 3. It might be interesting to know that the interannual variability, even on the seasonal time-scale, is pretty strong. For example, the September–November tropical rain maximum at 8°–10°N was about 18 units (1 g cm^{-2} $month^{-1}$) in the fall of 1973 but only about 12 units in the fall of 1974; the same maximum in the December–February season at 0°–5°N was 19 units in 1972–73, 8 units in 1973–74, and 13 units 1974–75. Concerning the ratio of the precipitation maximum in the tropics and the one in the extratropics the results of Rao *et al.* indicate that in general it is slightly greater than 1. However, in specific cases this can be as low as ½ (February 1975)

or even $\frac{1}{3}$ (January 1974). This supports the January pattern of our Fig. 3 which shows a ratio of about 1.

Fig. 4 presents the 1000 mb values of Fig. 2 for all months of the year in a time-latitude section. The rainbelts (>12.5 units) appear as shaded, the arid zones (<5.0 units) as stippled areas. This figure might be compared with Fig. 5.30 of Newell *et al.* (1972). The seasonal shift of the equatorial rainbelt is clearly visible. It should be remarked that the position of the maximum precipitation appears to be too far south for the period February–August. The subtropical region is arid only from November–May; the aridity appears to be removed in summer due to the influence of the monsoonal circulation.

6. Summary and conclusions

We have demonstrated the significance of the vertical precipitation flux PREC by zonal mean cross sections through the northern atmosphere. They show that PREC is a continuous function of height and latitude. It has sizeable downward directed values even at stratospheric levels and increases monotonically toward the earth's surface. Its primary maximum in meridional direction is located in the tropics, with a secondary in midlatitudes. The vertical structure of PREC is largely determined by the radiation term RAD and the meridonal structure is governed by the integrated divergence of the zonal mean potential heat flux vector ADV.

The net error of the present approach (± 10 W m^{-2}), most evident in extratropical latitudes in winter, is due to the following influences:

- Uncertainty of the radiation flux; RAD must be computed from models.
- Uncertainty of the MIT-Library data. Although these data have the highest possible standard, some uncertainty remains, presumably due to wind errors and uneven coverage.
- Uncertainty of the parameterization used for the vertical transient eddy heat flux.
- Uncertainty of the boundary layer flux which cannot be measured but must be estimated from bulk formulas.
- Differences between the earth's surface and 1000 mb level.

Hantel and Peyinghaus (1976) have grouped the various terms of Eq. (3.5) in a different order from that used here. The vertical flux components $g^{-1}[\overline{\omega s}]$, $[\overline{H_R}]$ and $L[\overline{H_C}]$ were combined into a generalized vertical heat flux F_p. Then F_p could be obtained from the first term of ADV, with $[\overline{H_R}]_{p=0}$ as a boundary condition at the top of the atmosphere. The advantage of this approach is that the three components of F_p, which are caused by physically different mechanisms, represent the total vertical heat flux across a given atmospheric level. The deficiency of this approach is that F_p turns out to be highly dependent upon a reference constant s_0 which represents the mean atmospheric heat content. In the present study this deficiency has been removed; the net advective term ADV is strictly independent upon any reference constant.

While RAD is fairly uniformly distributed in the meridional direction, PREC shows distinct maxima and minima due to ADV. The leading term in the definition (3.4) for ADV is the first. However, the horizontal heat flux divergence vanishes when averaged over all latitudes. Thus for the global and annual average, denoted by the tilde, Eq. (3.5) reduces to

$$\frac{1}{g}\widetilde{[\overline{\omega s}]}+\widetilde{\mathrm{RAD}}=\widetilde{\mathrm{PREC}}. \tag{6.1}$$

The first term is small compared to the other two. This is evident at the surface [mean Bowen ratio ≈ 0.35; see Sellers (1965)] and has been shown to apply also for the free atmosphere (Langholz, 1976). Thus it is justified to refer to the global heat budget as an approximate *radiative-precipitative equilibrium*. Recent studies in the tropics (e.g., Betts, 1975) imply a similar balance in precipitating mesoscale systems. It is hoped that the current tropical experiments, notably GATE, will further clarify the role of the precipitation flux in the free atmosphere.

Acknowledgments. Part of this study has been sponsored by the Deutsche Forschungsgemeinschaft, Grant Ha 839/3. The figures have been drawn by Miss B. Eggemann.

REFERENCES

Betts, A. K., 1975: Parametric interpretation of trade-wind cumulus budget studies. *J. Atmos. Sci.*, **32**, 1934–1945.

Budyko, M. I., 1963: *Atlas of the Heat Balance of the Earth.* Moscow, Gidrometeoizdat., 69 pp.

Falcóner, P. D., and W. Peyinghaus, 1975: Radiative balance in the atmosphere as a function of season, latitude, and height. *Arch. Meteor. Geophys. Bioklim.*, **B23**, 201–223.

Hantel, M., 1974: On the display of the atmospheric circulation with streamfunctions. *Mon. Wea. Rev.*, **102**, 649–661.

——, 1976: On the vertical eddy transports in the northern atmosphere. I. Vertical eddy heat transport for summer and winter. *J. Geophys. Res.*, **81**, 1577–1588.

——, and H.-R. Baader, 1976: On the vertical eddy heat flux in the northern atmosphere. *Beitr. Phys. Atmos.*, **49**, 149–167.

——, and W. Peyinghaus, 1976: Vertical heat flux components in the northern atmosphere. *Mon. Wea. Rev.*, **104**, 168–179.

——, D. Dedenbach and H. Hüster, 1976: Energy streamfunctions in the vertical-meridional plane for the northern atmosphere. *J. Atmos. Sci.*, **33**, 617–631.

Hare, F. K., and J. E. Hay, 1971: Anomalies in the large-scale annual water balance over northern north America. *Can. Geograph.*, **15**, 79–94.

Jaeger, L., 1976: Monatskarten des Niederschlags für die ganze Erde. *Ber. Dtsch. Wetterdienstes*, No. 139.

Kessler, E., 1969: On the distribution and continuity of water substance in atmospheric circulations. *Meteor. Monogr.*, No. 32, Amer. Meteor. Soc., 84 pp.

Langholz, H., 1976: Der Niederschlagsfluß in der freien Atmosphäre. Diploma thesis, Bonn, 66 pp.

Möller, F., 1951: Vierteljahrskarten des Niederschlags für die ganze Erde. *Petermann Geograph. Mitt.*, **95**, 1–7.

Newell, R. E., D. G. Vincent, T. G. Dopplick, D. Ferruzza, and J. W. Kidson, 1969: The energy balance of the global atmosphere. *Proc. Roy. Soc. London*, 42–90.

——, J. W. Kidson, D. G. Vincent and G. J. Boer, 1972: *The General Circulation of the Tropical Atmosphere, and Interactions with Extratropical Latitudes*, Vol. 1. The MIT Press, 258 pp.

——, ——, —— and ——, 1974: *The General Circulation of the Tropical Atmosphere, and Interactions with Extratropical Latitudes*, Vol. 2. The MIT Press, 371 pp.

Oort, A. H., 1971: The observed annual cycle in the meridional transport of atmospheric energy. *J. Atmos. Sci.*, **28**, 325–339.

Oort, A. H., and E. M. Rasmusson, 1971: Atmospheric circulation statistics. NOAA Prof. Pap. No. 5, 323 pp.

Peyinghaus, W., 1974: Eine numerische Berechnung der Strahlungsbilanz und die Strahlungserwärmung der Atmosphäre im Meridional-Vertikalschnitt. *Bonner Meteor. Abhandl.*, **22**, 63 pp.

Rao, M. S. V., W. V. Abbott III and J. S. Theon, 1976: Satellite-derived global oceanic rainfall atlas (1975 and 1974). Preprint X-911, 76–116, Goddard Space Flight Center, Greenbelt, Md. [Available from U. S. Government Printing Office.]

Saltzman, B., and A. D. Vernekar, 1971: An equilibrium solution for the axially symmetric component of the earth's macroclimate. *J. Geophys. Res.*, **76**, 1498–1524.

Sasamori, T., 1975: A statistical model for stationary atmospheric cloudiness, liquid water content, and rate of precipitation. *Mon. Wea. Rev.*, **103**, 1037–1049.

Schutz, C., and W. L. Gates, 1971: Global climatic data for surface, 800 mb, 400 mb. January (R-915-ARPA), April (R-1317-ARPA), July (R-1029-ARPA), and October (R-1425-ARPA). Rand Corp., Santa Monica, Calif.

Sellers, W. D., 1965: *Physical Climatology*. The University of Chicago Press, 272 pp.

Thommes, W., 1974: Die Bestimmung der zonal und zeitlich gemittelten Erwärmungsrate durch Kondensation aus dem 1. Hauptsatz. *Ann. Meteor. NF*, **9**, 41–43.

Van Mieghem, J., 1973: *Atmospheric Energetics*. Clarendon Press, 306 pp.